Electrodeposition of Cu(In,Ga)Se2 Crystals on High-Density CdS Nanowire Arrays for Photovoltaic Applications

ARTICLE *in* CRYSTAL GROWTH & DESIGN · NOVEMBER 2010

Impact Factor: 4.89 · DOI: 10.1021/cg101157a

4 AUTHORS, INCLUDING:

Sung-Hwan Han
Hanyang University
336 PUBLICATIONS **5,199** CITATIONS
SEE PROFILE

Yun-Mo Sung
Korea University
107 PUBLICATIONS **1,644** CITATIONS
SEE PROFILE

DOI: 10.1021/cg101157a

CRYSTAL GROWTH & DESIGN Article

2010, Vol. 10
5297–5301

Electrodeposition of Cu(In,Ga)Se_2 Crystals on High-Density CdS Nanowire Arrays for Photovoltaic Applications

Woo-Chul Kwak,[†] Sung-Hwan Han,[‡] Tae Geun Kim,[§] and Yun-Mo Sung*,[†]

[†]*Department of Materials Science & Engineering, Korea University, Seoul 136-713, South Korea,* [‡]*Department of Chemistry, Hanyang University, Seoul 133-791, South Korea, and* [§]*Department of Electronic Engineering, Korea University, Seoul 136-713, South Korea*

Received September 1, 2010; Revised Manuscript Received October 9, 2010

ABSTRACT: High-density and single-crystalline CdS nanowires were grown on fluorine-doped tin oxide (FTO)/soda-lime glass substrates using Bi catalysts via the so-called solution−liquid−solid (SLS) mechanism. Through a series of voltage loading steps, high-quality Cu(In,Ga)Se_2 (CIGS) light absorption layers were electrochemically deposited on the CdS window layers and subsequently selenized at 400 °C to form photovoltaic cells. Due to the one dimensionality and single crystallinity of the CdS nanowires, the carrier collection efficiency could be improved. The resulting CIGS/CdS nanowire solar cells showed a light energy conversion efficiency of ∼6.18% under AM 1.5 conditions (I = 100 mW/cm^2), which is ∼28.7% higher than that of the equivalent CIGS solar cells containing chemically deposited CdS thin film as a window layer.

1. Introduction

Chalcopyrite solar cells have lately become a subject of special interest, since chalcopyrite compounds show strong optical absorption and stability against photodegradation. Moreover, their lattice constants and energy band gaps can be easily tailored by modifying the elemental composition of the compounds. Light energy conversion efficiencies of almost 20% have been reported for lab-scale chalcopyrite solar cells.[1,2]

More recently, solar cells based on nanowires or nanorods have been highlighted as one of the most efficient forms, because their nanoscale structures endow them with various advantages, such as superior optical, electrical, and chemical properties caused by their single crystallinity, size confinement, increased surface-to-volume ratio, etc.[3−9] Using nanowire structures, it is possible to obtain a low exciton recombination rate, leading to high collection efficiency due to the remarkably increased p−n junction area and the reduced carrier paths. In addition to these properties, the single crystallinity of nanowires permits the solar cells to induce a higher photocurrent and, consequently, higher efficiency compared with other superstrate cells based on polycrystalline thin film or bulk structures.[10−12]

Although there have been several reports on nanowire solar cells, they have been mainly limited to organic dye-sensitized solar cells (DSSCs). In the case of inorganic-phase absorber films, Yang et al. recently reported the use of nanowires overcoated with an oxide film.[11] However, their method seems difficult to apply in practice, because subsequent vacuum annealing of the nanoparticles is required in the fabrication process.

Several methods of fabricating CIGS films exist, such as coevaporation, sputtering, pyrolysis, and electrodeposition.[13−16] Among these, electrodeposition can provide cost-effective and large-scale fabrication of CIGS films. In this study, using controlled electrodeposition methods, we were able to deposit a high-density CIGS absorber film from the top to the bottom of the nanowires to form photovoltaic cells.

2. Experimental Section

All chemicals were purchased from Sigma-Aldrich and used as received. Fluorine-doped tin oxide (FTO) was purchased from Libbey−Owens−Ford (TEC 8, 75% transmittance in the visible spectrum). CdS nanowires on FTO electrodes were prepared using a solution−liquid−solid (SLS) mechanism.[17−19] Cadmium oxide (99.99%, 0.05 mmol), 0.5 mL of oleic acid, 20 mg of hexadecylamine (98%), 150 mg of trioctylphosphine oxide (TOPO, 99%), and 8 mL of 1-octadecene (ODE) were loaded in a 100 mL three-neck flask. The mixture solution was heated to 220 °C under Ar gas flowing with stirring. A CdS layer with a thickness of ∼40 nm was deposited onto the FTO substrates by sputtering. Subsequently, a thin layer of Bi with a thickness of ∼5 nm was coated on the CdS layer by DC sputtering. Then, the FTO substrates bearing the Bi catalyst layer were dipped into poly(vinyl alcohol) (PVA) solution to produce a PVA protection layer on the Bi catalysts. The PVA/Bi/CdS/FTO/soda-lime glass substrates were heat treated at 220 °C for 1 h under Ar flow in a tube furnace to break the Bi layer into Bi nanoparticles, in order for them to serve as catalysts for the nucleation of the CdS nanowires. After the electrodes bearing the Bi catalysts were loaded into the flask containing the prepared solution, 0.5 mL of 5 wt % sulfur−tertiary butyl phosphine (TBP) solution was additionally injected into the solution, and the reaction was continued for 4 h under gentle stirring or without stirring. The solution was cooled to room temperature, and the resulting samples with high-density CdS nanowires were rinsed with chloroform.[9]

CIGS thin films were electrodeposited on CdS nanowire/FTO glass at room temperature using a three-electrode potentiostatic system with a saturated Ag/AgCl electrode as a reference electrode and a platinum plate (1 cm^2) as a counter electrode. The electrodeposition of the CIGS films was performed using the chronoamperometry mode (−0.3, −0.5, and −0.7 V versus Ag/AgCl) in which the deposition potential is fixed for 2 min for the measurement of the reverse-FE current samples and 60 min for the photovoltaic device samples. The concentration of the precursor solutions was selected to be 2.5 mM for $CuCl_2$, 2.5 M for $InCl_3$, 5.7 mM for $GaCl_3$, and 4.5 mM for H_2SeO_3, each of which was adjusted to a pH of 1.5 (±0.1) using 0.1 M HCl solution. In addition, 0.24 M LiCl was used as a supporting electrolyte.[20] The thermal annealing of the as-deposited CIGS films was performed at 400 °C for 15 min in a selenium atmosphere for the so-called selenization process. The CIGS films

*To whom correspondence should be addressed. E-mail: ymsung@korea.ac.kr. Tel: 82-2-3290-3286. Fax: 82-2-928-3584.

Published on Web 11/15/2010

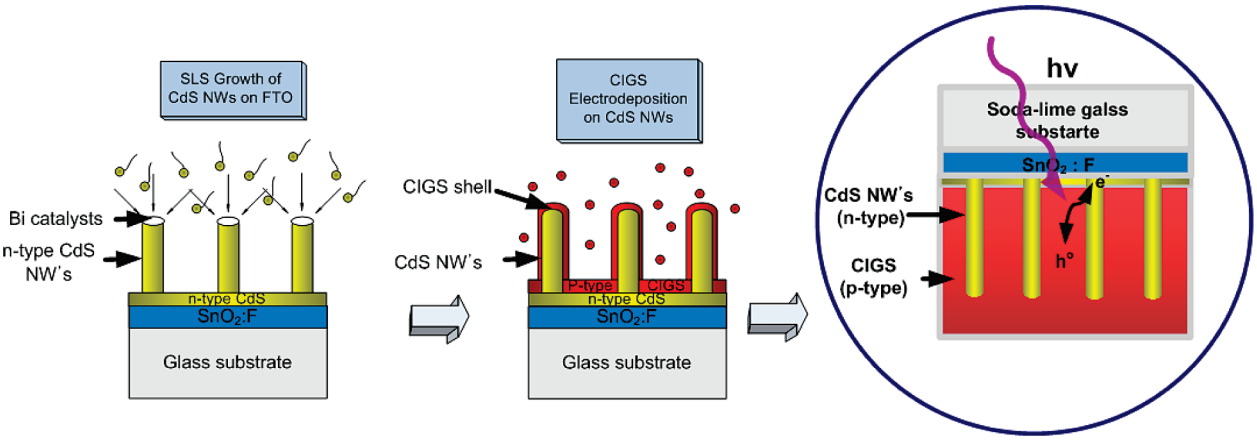

Figure 1. Schematic diagram showing the procedure for CdS nanowire growth and CIGS electrodeposition to make CIGS/CdS solar cells.

obtained were subsequently etched in a 10% KCN aqueous solution for 5 min to remove any possible secondary phases. For comparison, reference photovoltaic cells of CIGS/CdS film were fabricated using a procedure identical to that for CIGS/CdS nanowire cells except for the voltage loading. The CIGS layer was electrodeposited on CdS film/FTO substrates at a constant voltage of −0.7 V.

The variation in the morphological features of the CIGS crystals and films during deposition were monitored using scanning electron microscopy (SEM). Also, the chemical compositions of the films were analyzed using energy-dispersive X-ray spectroscopy (EDS). The crystallinity of the samples was investigated using X-ray diffraction (XRD). High-resolution transmission electron microscopy (HRTEM) was employed to investigate the crystallinity and morphological features of the samples.

For the performance measurement of the photovoltaic devices, Au was evaporated onto the CIGS/CdS/FTO substrates at a pressure of $< 10^{-6}$ Torr. The photovoltaic devices were irradiated by 100 mW/cm^2 white light with air mass (AM) 0 and 1.5 filters as a solar simulator (450 W xenon lamp, Oriel Instruments), and the current was measured with a Keithley 2400 source meter. Figure 1 presents a schematic diagram showing the procedure for CdS nanowire growth and CIGS layer electrodeposition.

3. Results and Discussion

CdS nanowires were synthesized on CdS/FTO/soda-lime glass substrates by liquid-phase growth for use as a window layer. A thin CdS layer with ∼40 nm thickness was deposited on FTO/soda-lime glass substrates by sputtering for the purpose of inducing the homoepitaxial growth of CdS nanowires and completely overcoating the FTO electrode. The single-crystalline CdS nanowires with a diameter and length of ∼50−100 nm and ∼2−5 μm, respectively, were formed at 220 °C within 4 h. Due to the low melting temperature of 271 °C, Bi catalysts in a nanoparticle shape could easily form by thermal breakage of a Bi thin layer precoated on CdS/FTO/soda-lime glass. We could successfully keep the nanoscale Bi catalysts at the surface of CdS/FTO/soda-lime due to the PVA adhesion layer. The Bi catalysts forming low eutectic temperatures with alloying elements such as Cd and S played a decisive role in lowering the process temperature of the SLS growth of CdS nanowires. The detailed method and mechanism are described in our previous report.[9]

To obtain a dense CIGS film, a series of voltage loadings (−0.3, −0.5, and −0.7 V) were used. In general, the applied potential for the deposition of CIGS ranges from −0.6 to −0.8 V, because the highest standard potential gap of Ga^{3+} to Ga is about −0.75 V (SCE), which is the process requirement for the Ga inclusion in CIGS with maintaining high crystallinity of CIGS. However, this potential range seemed to be inadequate for achieving a highly compact film in our case. When a high potential was applied to the system, it was difficult to fill the inner spaces with a size of ∼200 nm between the CdS nanowires. This is due to the large CIGS particle size caused by the high deposition rate of the ions. Thus, through a series of voltage loadings, we could obtain a highly compact CIGS layer filling the spaces between the CdS nanowires and also overcoating the CdS nanowire layer. The gradual change in the morphological features of samples according to electrodeposition voltage and time was monitored by field emission electron microscopy (FESEM) analyses, as shown in Figure 2. Figure 2a shows the dense electrodeposited film formed under the CdS nanowires in the case where the applied voltage and time were −0.3 V and 1 min, respectively. Under these conditions, mainly Cu^{2+} (0.12 V to Cu vs SCE) and Se^{4+} (0.52 V to Se vs SCE) ions could take part in the reaction, and therefore, a Cu_2Se compound could form on the FTO substrate. Despite the absence of formation of Ga^{3+} and Se^{4+} ions, this pretreatment was considered to be important for the formation of a compact film, as mentioned above. In more detail, this low potential load allowed the inner space between the small nanoparticles to be effectively filled and few pores to be produced. As the process time increases to 10 and 20 min at the same voltage, Cu_2Se nanoparticles with size of ∼30−50 nm were deposited at the bottom and on the nanowire surface at the same time, as shown in Figure 2b,c. The film surface consists of a smooth and dense layer and the nanoparticles. After pretreatment for 20 min, electrodeposition was performed for 20 min at −0.5 V, and the image of the resulting film is depicted in Figure 2. This voltage was applied to reduce the stress built up between the Cu_2Se and CIGS. An abrupt increase in potential can induce stress and cause the Cu_2Se film to contain In (−0.55 V from In^{3+} to In vs SCE) element due to the reduction half-reaction. The particle size is approximately 200 nm, and this is not appropriate to produce a compact film, as mentioned above. Finally, a voltage of −0.7 V was applied for 20 min to realize the CIGS system. The film consists of very dense CIGS grains with average size of ∼200 nm, as shown in Figure 2e. Figure 2f shows the cross-sectional image of CIGS/CdS films after selenization. The thickness of the CIGS layer was ∼3 μm, and the film was dense and pore free. Figure 3 shows the TEM and HRTEM images of CdS nanowires and attached Cu_2Se particles. The CdS nanowires were single crystalline, and the crystal growth orientation was identified as [002]. The fringe image of Cu_2Se

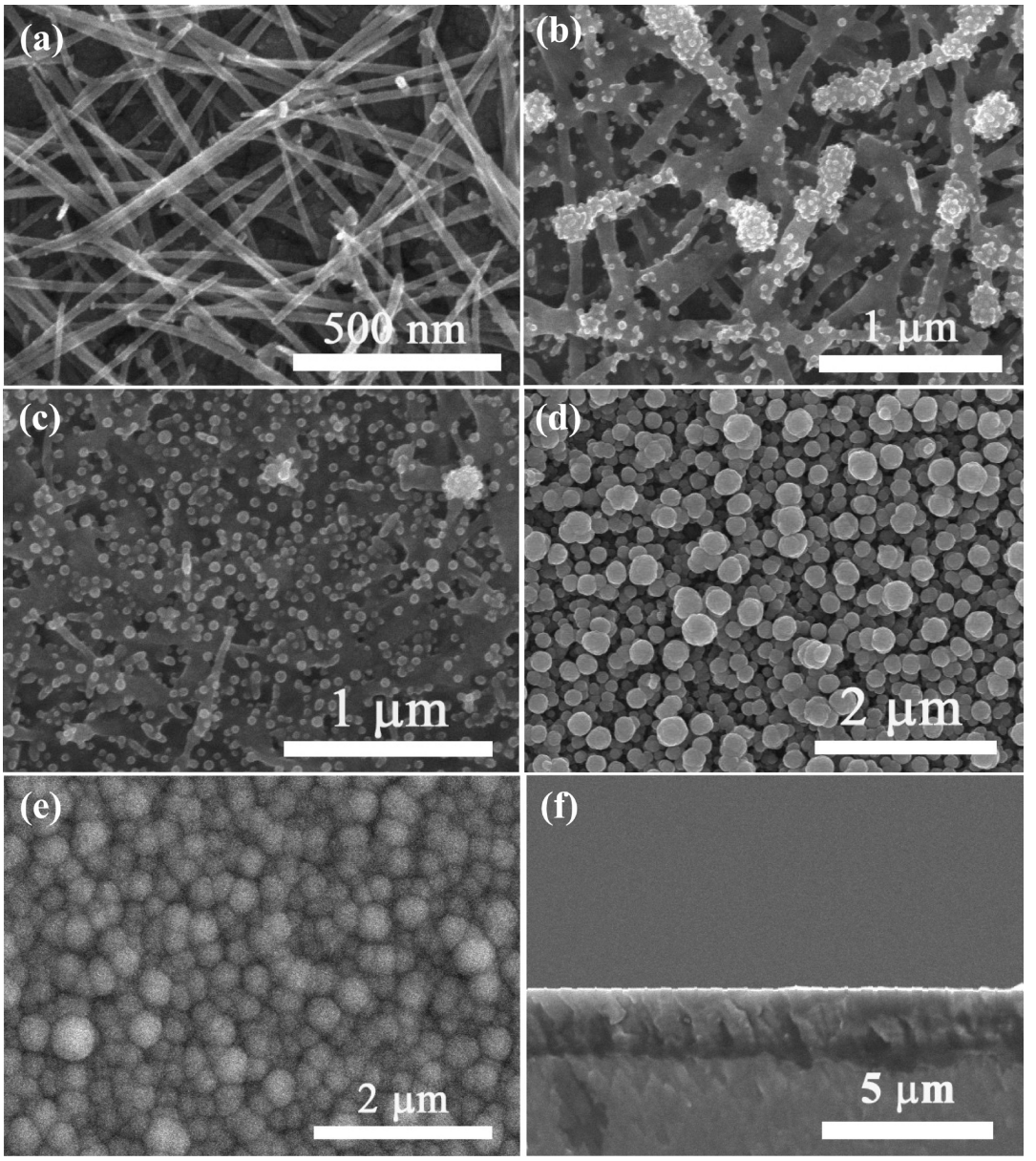

Figure 2. SEM plan-view images showing the progress in CIGS film formation at the CdS nanowire/FTO substrates. The processing conditions were (a) −0.3 V and 1 min, (b) −0.3 V and 10 min, (c) −0.3 V and 20 min, (d) −0.5 V and 20 min, and (e) −0.7 V and 20 min. Panel f shows a SEM cross-sectional image of the final CIGS film after the selenization process.

was obscure, and it is most likely that the crystallinity of Cu_2Se was not high at the electrodeposition stage.

After selenization treatments, the average chemical composition of the films were determined to be $Cu_{1.23}In_{0.65}Ga_{0.35}Se_2$ using EDS analyses. The initial Cu_2Se crystals were converted to the CIGS phase after the selenization. During selenization treatment at 400 °C, In and Ga diffusion into the Cu_2Se crystals could be completed to form the CIGS phase, since the size of Cu_2Se crystals is about 200 nm, and thus the diffusion path is only 100 nm. As for the reference sample of CIGS/CdS film, the final chemical composition after selenization was $Cu_{1.12}In_{0.61}Ga_{0.39}Se_2$, very close to the CIGS/CdS nanowires. Also, the thickness of the CIGS layer was 3 μm, identical to the CIGS/CdS nanowire samples. The average grain size of the CIGS/CdS nanowire and CIGS/CdS film samples was 250 and 280 nm, respectively (See Supporting Information, section SI-1). Slight grain growth occurred in the electrodeposited CIGS films during the selenization annealing at 400 °C. The CIGS films showed the characteristic X-ray diffractions (XRD) such as (224/220) and (312/116), which are in good agreement with the tetragonal structure listed in the JCPDS reference [35-1102] (Figure 4). However, the (112) diffraction peak of the CIGS films was overlapped with that of CdS (002). The XRD patterns of CIGS on the electrode show that it is obviously crystalline and stoichiometric, which implies that it can serve for photovoltaic devices with high power conversion efficiency. However, the relative intensity of the diffraction peaks from the CIGS phase was not high compared with that from the CdS nanowires, which would come not from the low crystallinity of the CIGS film but from the strong diffraction from the preferential growth atomic planes such as (002) of CdS nanowires. The absolute diffraction intensity of CIGS film was not low. The diffraction patterns and intensity were almost identical to the CIGS/CdS film samples.

In order to confirm that the CIGS/CdS/FTO samples are working properly as photovoltaic devices, $I-V$ measurements

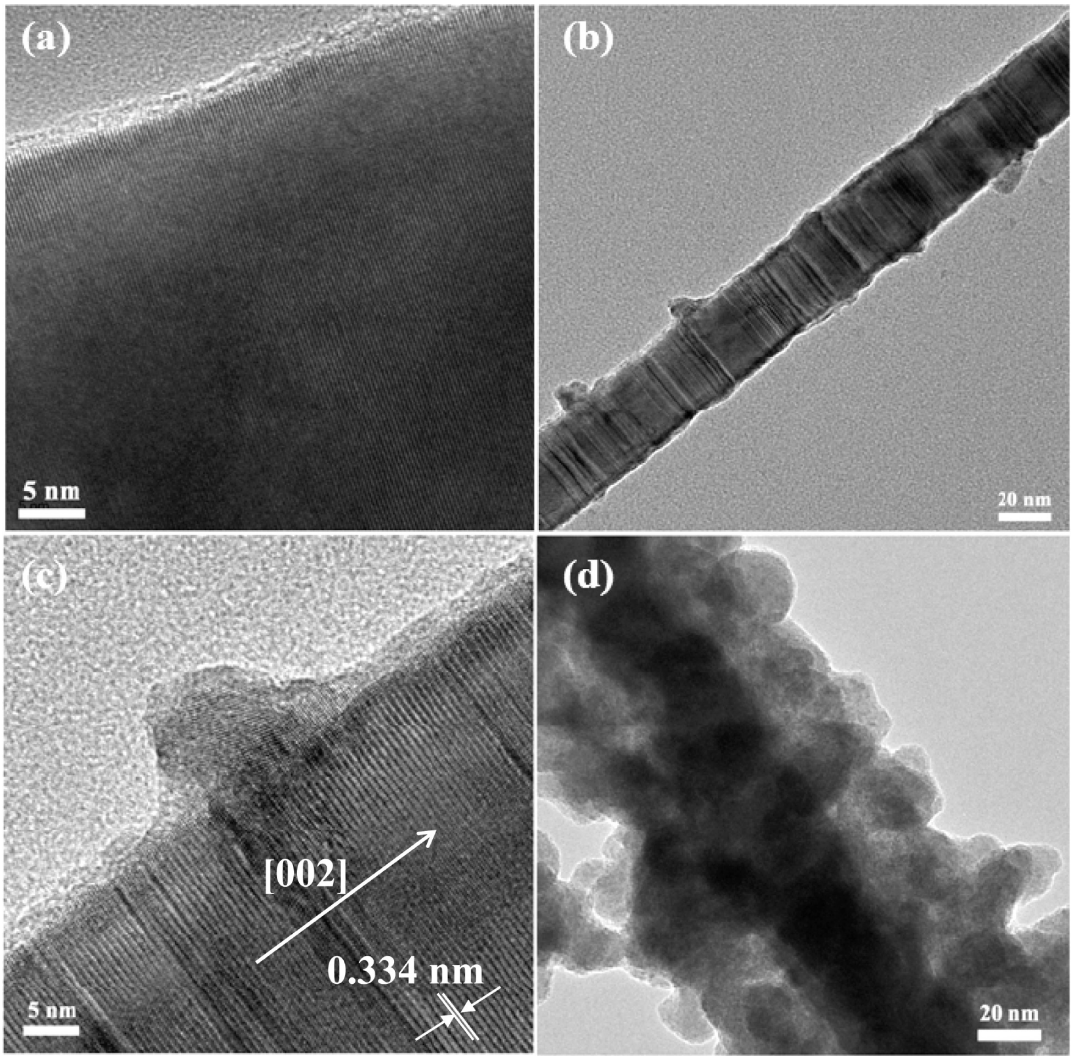

Figure 3. TEM images of (a) CdS nanowires grown on FTO glass substrates, (b) Cu_2Se attached to CdS nanowires at −0.3 V for 1 min, HRTEM images of (c) the structures in panel b and (d) those deposited at −0.3 V for 10 min.

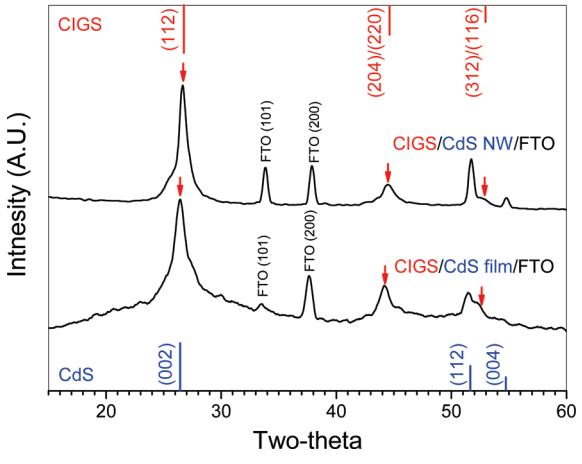

Figure 4. XRD pattern of CIGS/CdS nanowire/FTO substrates prepared via electrochemical deposition, compared with that of CIGS/CdS film/FTO substrates. The red arrows indicate the diffraction from the CIGS phase.

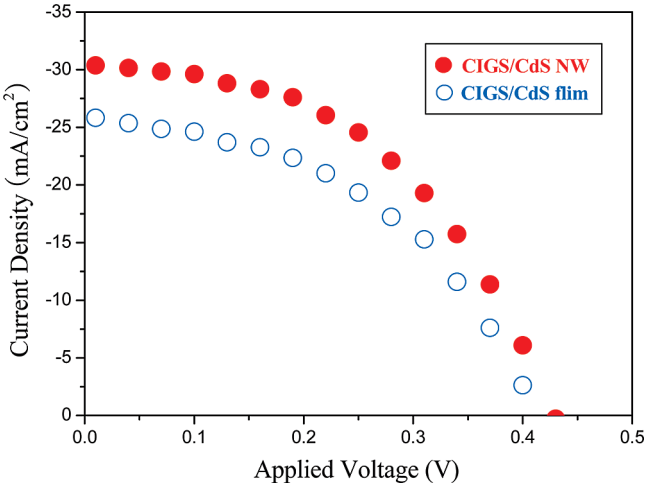

Figure 5. Comparison of the photocurrent density−voltage ($J-V$) characteristics between the CIGS/CdS nanowire cells and CIGS/CdS bilayer film cells.

were carried out. The $I-V$ characteristics and photovoltaic performances of the CIGS photovoltaic devices with the CdS nanowires and CdS films under light illumination are shown and compared in Figure 5 and Table 1, respectively. The CIGS photovoltaic devices with the CdS nanowires showed a power conversion efficiency (E_{ff}) of 6.18% with a short-circuit

Table 1. Comparison of Chemical Composition, Open-Circuit Voltage (V_{oc}), Short-Circuit Photocurrent Density (J_{sc}), Fill Factor (ff), and Efficiency (%) between the CIGS/CdS NW Cells and CIGS/CdS Bilayer Film Cells

cells	composition	V_{oc} (V)	J_{sc} (mA/cm^2)	ff	E_{ff} (%)
CIGS/CdS film	$Cu_{1.23}In_{0.65}Ga_{0.35}Se_2$	0.41	26.05	0.45	4.80
CIGS/CdS NW	$Cu_{1.12}In_{0.61}Ga_{0.39}Se_2$	0.43	30.06	0.47	6.18

current (J_{sc}) = 30.06 mA/cm^2, open-circuit voltage (V_{oc}) = 0.43 V, and fill factor (ff) = 0.47. On the other hand, the CIGS photovoltaic devices with the chemically deposited CdS films exhibited an E_{ff} of 4.80% with a J_{sc} of 26.5 mA/cm^2, V_{oc} of 0.41 V and ff of 0.45. The superstrate-type CIGS cells with the CdS nanowires showed high power conversion efficiency, due to the apparently enhanced J_{sc}, which is attributed to the one-dimensional structure and single crystallinity of the CdS nanowires in the photovoltaic cells. The layers of CdS nanowires in the photovoltaic cells increased the interface area. Considering the 12% growth density of the CdS nanowires with average diameter of 75 nm and length of 3.5 μm, the CIGS/CdS nanowire structure has about 23 times larger interfacial area than the CIGS/CdS film structure. However, more trapping of charge carriers at the increased interfacial area could occur as well, and as a result, the power conversion efficiency of the superstrate-type CIGS photovoltaic cell was increased by 28.7% in the presence of the CdS nanowires.

4. Conclusions

High-density and single-crystalline CdS nanowires were grown at the surface of FTO/soda-lime glass substrates via low-temperature liquid-phase synthesis, the solution−liquid−solid (SLS) mechanism. By employing electrochemical deposition with a series of voltage loadings, we could successfully deposit a compact CIGS layer over high-density CdS nanowires. The photovoltaic cells with CdS nanowires showed improved light energy conversion efficiency compared with those with CdS film. Our approach strongly suggests the possibility of large-scale and low-cost production of high-efficiency CIGS solar cells based upon nanowire structures via mild wet chemistry.

Acknowledgment. This work was supported by the National Research Foundation of Korea (NRF) grant funded by the Korea government (MEST) (2010-0015876). This work was also supported by Korea-International Cooperative Research and Development Project (2009) between Korea and Central Asia funded by Ministry of Knowledge Economy (MKE).

Supporting Information Available: FESEM images of selenized CIGS/CdS nanowire and CIGS/CdS film samples and energy band structure of CIGS/CdS. This material is available free of charge via the Internet at http://pubs.acs.org.

References

(1) Moreels, I.; Lambert, K.; De Muynck, D.; Vanhaecke, F.; Poelman, D.; Martins, J. C.; Allan, G.; Hens, Z. *Chem. Mater.* **2007**, *19*, 6101.
(2) Contreras, M. A.; Egaas, B.; Ramanathan, K.; Hiltner, J.; Swartzlander, A.; Hasoon, F.; Noufi, R. *Prog. Photovoltaics* **1999**, *9*, 311.
(3) Rothschild, A.; Levakov, A.; Shapira, Y.; Ashkenasy, N.; Komem, Y. *Surf. Sci.* **2003**, *532*, 456.
(4) Appell, D. *Nature* **2002**, *419*, 553.
(5) Park, N.-G.; Van de Lagemaat, J.; Frank, A. J. *J. Phys. Chem. B* **2000**, *104*, 8989.
(6) Xia, Y. N.; Yang, P. D.; Sun, Y. G.; Wu, Y. Y.; Mayers, B.; Gates, B.; Yin, Y. D.; Kim, F.; Yan, Y. Q. *Adv. Mater.* **2003**, *15*, 353.
(7) Lee, J.-C.; Kim, T. G.; Lee, W.; Han, S.-H.; Sung, Y.-M. *Cryst. Growth Des.* **2009**, *9*, 4519.
(8) Lee, J.-C.; Lee, W.; Han, S.-H.; Kim, T. G.; Sung, Y.-M. *Electrochem. Commun.* **2009**, *11*, 231.
(9) Kwak, W.-C.; Kim, T. G.; Lee, W.; Han, S.-H.; Sung., Y.-M. *J. Phys. Chem. C* **2009**, *113*, 1615.
(10) Cahen, D.; Hodes, G.; Gratzel, M.; Guillemoles, J. F.; Riess, I. J. *Phys. Chem. B* **2000**, *104*, 2053.
(11) Yuhas, B. D.; Yang, P. D. *J. Am. Chem. Soc.* **2009**, *131*, 3756.
(12) Wang, Q.; Zhu, K.; Neale, N. R.; Frank., A. J. *Nano Lett.* **2009**, *9*, 806.
(13) Repins, I.; Contreras, M. A.; Egaas, B.; DeHart, C.; Scharf, J.; Perkins, C. L.; To, B.; Noufi, R. *Prog. Photovoltaics* **2008**, *16*, 235.
(14) Hall, A. J.; Hebert, D.; Lei, C.; Ockett, A.; Siebentritt, S. *J. Appl. Phys.* **2008**, *103*, No. 083540.
(15) Kaelin, M.; Rudmann, D.; Tiwari, A. N. *Sol. Energy* **2004**, *77*, 749.
(16) Fernandez, A. M.; Bhattacharya, R. N. *Thin Solid Films* **2005**, *474*, 10.
(17) Wang, F. D.; Buhro, W. E. *Small* **2010**, *6*, 573.
(18) Wang, F. D.; Dong, A. G.; Sun, J. W.; Tang, R.; Yu, H.; Buhro, W. E. *Inorg. Chem.* **2006**, *45*, 7511.
(19) Ouyang, L.; Maher, K. N.; Yu, C. L.; McCarty, J.; Park, H. *J. Am. Chem. Soc.* **2007**, *129*, 133.
(20) Calixto, M. E.; Dobson, K. D.; McCandless, B. E.; Birkmire, R. W. J. *Electrochem. Soc.* **2006**, *153*, G521.